

The best least-squares fit straight line has been passed through the experimental points, yielding

$$A_0^+ = (1.51 \pm 0.14) \times 10^{-29}; \quad A_2^+ = (1.12 \pm 0.31) \times 10^{-29}.$$

The errors are determined by a weighted propagation of the errors of the individual observations. Consideration of the external consistency of the points leads to the same estimated errors. The value of  $A_0^+$  gives directly the following total cross section for  $S$ -wave

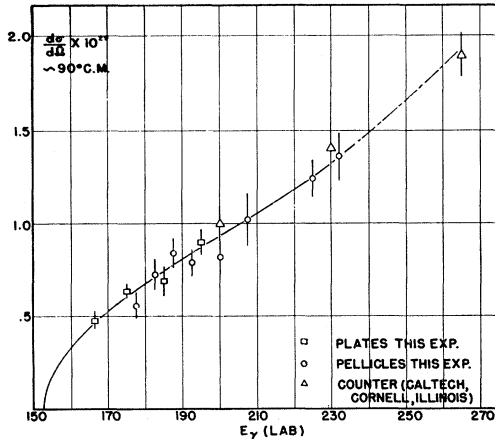


FIG. 1. The  $90^\circ$  c.m. cross section for photoproduction of pions in hydrogen versus photon energies in the laboratory frame. The solid curve was obtained by transformation of the straight line of Fig. 2.

photoproduction at threshold:

$$e.m. \sigma^{+S \text{ wave}} = (1.90 \pm 0.18) \times 10^{-28} \chi. \quad (4)$$

A theorem due to Kroll and Ruderman<sup>4</sup> proves, for a relativistic covariant meson theory, that at threshold,<sup>5</sup>

$$A_0^\pm = \frac{e^2 g^2}{2M^2} \left\{ 1 \pm \frac{\mu}{M} C + \left( \frac{\mu}{M} \right)^2 D \left( \frac{\mu}{M} \right)^\pm + \dots \right\}, \quad (5)$$

where  $e^2 = 1/137$ ,  $g$  is the renormalized symmetric coupling constant,  $\mu/M$  = ratio of pion mass to nucleon mass,  $C$  is a constant, and  $D^\pm$  are functions of  $\mu/M$ .

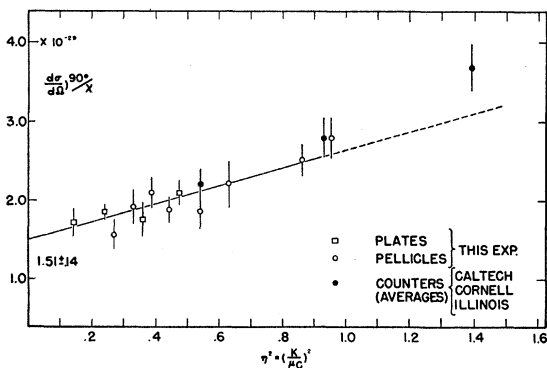


FIG. 2. Plot of  $(d\sigma/d\Omega)/\chi$  (see text) versus the square of pion momentum in the c.m. frame. The straight line represents the least-squares fit of the points of *this* experiment.

Thus if the assumption is made that  $(\mu/M)^2 D$  is negligible, it is found that

$$e^2 g^2 / 2M^2 = \frac{1}{2} (A_0^+ + A_0^-) = \frac{1}{2} A_0^+ (1 + A_0^- / A_0^+). \quad (6)$$

The ratio  $A_0^- / A_0^+$  is simply the limiting value at threshold of the ratio  $d\sigma(\pi^-) / d\sigma(\pi^+)$  from free nucleons. Available experimental data<sup>6</sup> indicate that this ratio in deuterium is  $1.51 \pm 0.1$ . This value requires some correction for the effects of the difference of the final states (alternatively two protons or two neutrons for the negative or positive pion case), but it is felt that the corrections will be no larger than the indicated limit of error.

Using this value for  $A_0^- / A_0^+$ , it is found that  $g^2 = 11.8 \pm 0.14$ .

Similarly the Chew cut-off theory gives, at threshold,

$$A_0^\pm = \frac{2e^2 f^2}{\mu^2} \left( 1 \pm \frac{\mu}{M} C' \right),$$

where  $f$  is the coupling constant for this theory. The value obtained is  $f^2 = 0.066 \pm 0.008$ .

We wish to express our deep appreciation to Professor A. O. Hanson for the continuous interest and invaluable help he has lent us throughout this work, and to Professor G. F. Chew and Professor F. Low for numerous enlightening discussions.

<sup>1</sup> G. Bernardini and E. L. Goldwasser, Phys. Rev. **94**, 729 (1954).

<sup>2</sup> P. D. Edwards and D. W. Kerst, Rev. Sci. Instr. **24**, 490 (1953).

<sup>3</sup> Jenkins, Luckey, Palfrey, and Wilson, Phys. Rev. (to be published); J. E. Leiss and C. S. Robinson (private communication); Bacher, Peterson, Tollestrup, and Walker (private communication).

<sup>4</sup> N. M. Kroll and M. A. Ruderman, Phys. Rev. **93**, 239 (1954).  
<sup>5</sup> Here the authors have assumed that the kinematical correction factors introduced in (1) are applicable to the Kroll-Ruderman theorem for the case  $\mu/M \neq 0$ .

<sup>6</sup> Beneventano, Lee, and Stoppini, Nuovo cimento (to be published); Sands, Teasdale, and Walker, Phys. Rev. (to be published).

## Decay Curve of $K$ Particles\*

L. MEZZETTI† AND J. W. KEUFFEL‡

Palmer Physical Laboratory, Princeton University,  
Princeton, New Jersey

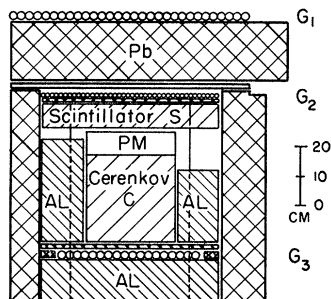
(Received June 14, 1954)

WE have measured the decay curve of stopped unstable cosmic-ray particles with liquid scintillators and directional Čerenkov counters.<sup>1</sup> Auxiliary information is provided by Geiger counters connected to an 80-channel hodoscope. The apparatus is shown in Fig. 1. Each Čerenkov counter is a hollow Lucite box filled with water, painted black on the bottom, and viewed from above by an RCA C7157 photomultiplier. The measured efficiency is 90 percent for fast  $\mu$  mesons traveling towards the photomultiplier end, and 0.4 percent for particles traversing the counter in the

opposite sense. The experimentally verified Čerenkov velocity threshold for water corresponds to  $E/mc^2 \geq 0.52$ .

The apparatus was designed to select events of the following type. A charged unstable particle produced in the generating layer of Pb passes through the scintillator *S* and stops near or inside one of the Čerenkov counters

FIG. 1. Experimental arrangement.  $G_1$  and  $G_3$  are trays of GM counters of diameter 1 in. and sensitive length 24 in.;  $G_2$  is a tray of  $\frac{1}{2}$ -in. GM counters of the same length. All the elements in the array are approximately square except for *S*, which is 11 in. by 24 in. There are two Čerenkov counters, one behind the other, each 1 ft square by 6 in. thick.



*C*. There it decays at rest into an upward-going relativistic secondary which is detected in *C* unobscured by downward-going shower particles. The time delay is measured with a 17-channel chronotron-type timing circuit.<sup>2,3</sup> The triggering requirements included the firing of any two counters in the  $G_2$  bank. We also later rejected, by examining the hodoscope pictures, events where an extension tray and/or tray  $G_1$  indicated an air shower and certain other events discussed below.

Our results are shown in Fig. 2. The time distribution shows a central peak and a well-defined exponential "tail" beginning at about 12.4  $\mu\text{sec}$ . If the lags greater than 12.4  $\mu\text{sec}$  are analyzed by the method of Peierls on the basis of a single exponential, the mean life is  $8.7 \pm 1.0 \mu\text{sec}$ . The systematic error is probably no larger than the statistical error quoted. The rate of such events, extrapolated to zero time, is  $3.5 \text{ hr}^{-1}$ .

Instrumental timing errors were studied in detail by inverting the Čerenkov counters and triggering on fast  $\mu$  mesons and soft showers. The timing error distributions were consistent with the shape of the central peak in Fig. 2, but could not possibly account for the exponential tail. We found, however, that large pulses in the scintillator—as indicated by a high multiplicity in a hodoscoped Geiger tray below it—produced a shift of 3 to 5  $\mu\text{sec}$  in the direction of apparent lags in the Čerenkov counters.<sup>4</sup> For this reason, we rejected events in the actual run where more than six counters were discharged in trays  $G_2$  or  $G_3$ .

Time lags might arise from differences in time of flight of two associated particles. We tested this possibility by displacing the Čerenkov counters 50 cm to one side, but still maintaining similar thicknesses of Pb above and around it. The rate of lags greater than 12.4  $\mu\text{sec}$  decreased by a factor of 20 under these conditions. (See "KB," Fig. 2.) Such a sharp decoherence cannot be associated with particles from a distant origin. We also verified with a neutron source

that the Čerenkov counters had a negligible response to neutrons.

The delayed events are most reasonably interpreted in terms of bona fide decays. Many short-lived unstable particles are known, but we wish to re-emphasize that we detect only those which produce relativistic secondaries. Thus  $\tau$  mesons can be detected only by the materialization of  $\gamma$  rays from the (relatively infrequent) alternative mode of decay  $\tau' \rightarrow \pi + 2\pi^0$  while the  $\pi \rightarrow \mu \rightarrow e$  process will be detected only by the decay electrons. These are distributed in time over a 2.2- $\mu\text{sec}$  mean life and are very inefficient in triggering the apparatus compared to long-range  $\mu$  mesons from *K* decay. A small number of lags in the microsecond range were indeed observed, but it was not possible in the present experiment to analyze these into 2.2- $\mu\text{sec}$  and flat random noise components; we can only say that the background from such events is at most about 0.5 counts per channel in Fig. 2. (If this background were doubled it would decrease the mean life by only 0.25  $\mu\text{sec}$ .)

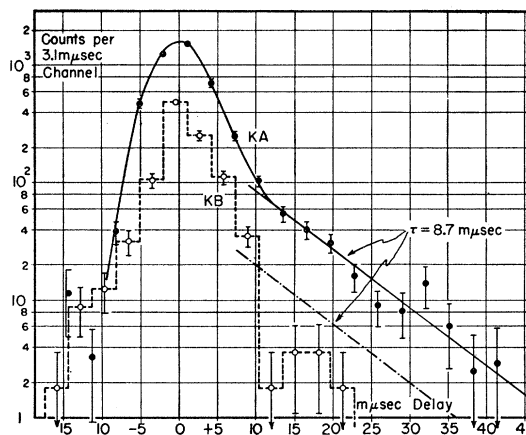


FIG. 2. Time lag distributions. *KA*: regular run, disposition as in Fig. 1, running time 230.7 hr, total rate  $19.8 \text{ hr}^{-1}$ . *KB*: test for lags due to time of flight. Čerenkov counters displaced 50 cm. Normalized to same running time as *KA*, so that differences in absolute rate of lags are significant.

The fact that we considered only lags greater than 12.4  $\mu\text{sec}$  in the analysis biases us strongly against processes with mean lives less than about 4  $\mu\text{sec}$ . Our results should be compared particularly with the results of the Paris cloud-chamber group,<sup>5</sup> where the minimum time of flight to the lower chamber is 5  $\mu\text{sec}$ . These investigators found a predominant *K* process  $K_\mu \rightarrow \mu + \nu$ , with a unique secondary momentum 223 Mev/*c*, and it appears likely that we are observing this particle. The Paris group<sup>6</sup> estimates the  $K_\mu$  mean life as 28  $\mu\text{sec}$ , but this value is not considered inconsistent with ours because of their small statistical sample. Earlier cloud-chamber mean life estimates gave lower and upper bounds of 4 and 10  $\mu\text{sec}$ .<sup>7,8</sup> In addition to the  $K_\mu$ 's, these estimates probably involved other

$K$  particles with mean lives short enough not to show up after 12.4  $m\mu\text{sec}$ .

Our rates appear to be consistent with cloud chamber and emulsion rates, but large uncertainties are involved in the comparison.

\* Sponsored by the joint program of the U. S. Office of Naval Research and the U. S. Atomic Energy Commission.

† On leave of absence from the University of Rome, Rome, Italy.

‡ Now at University of Utah, Salt Lake City, Utah.

<sup>1</sup> J. Winckler and K. Anderson, Rev. Sci. Instr. **23**, 765 (1952).

<sup>2</sup> J. W. Keuffel, Rev. Sci. Instr. **20**, 197 (1949).

<sup>3</sup> Keuffel, Harrison, Godfrey, and Reynolds, Phys. Rev. **87**, 942 (1952).

<sup>4</sup> Pulse heights could not be measured directly in this experiment because of amplifier saturation.

<sup>5</sup> Gregory, Lagarrigue, Leprince-Ringuet, Muller, and Peyrou, Nuovo cimento **11**, 292 (1954).

<sup>6</sup> B. Gregory, at Padua Conference on Heavy Mesons, April, 1954 (unpublished).

<sup>7</sup> Astbury, Buchanan, Chippindale, Millar, Newth, Page, Rytz, and Sahiar, Phil. Mag. **44**, 242 (1953).

<sup>8</sup> Bridge, Peyrou, Rossi, and Safford, Phys. Rev. **90**, 921 (1953).

## Energy Levels of $\text{Al}^{26}\dagger$

CORNELIUS P. BROWNE

Physics Department and Laboratory for Nuclear Science,  
Massachusetts Institute of Technology, Cambridge, Massachusetts  
(Received June 14, 1954)

IT has been pointed out<sup>1</sup> that the  $\text{Al}^{26}$  nucleus is of considerable interest from the standpoint of charge independence of nuclear forces and the isobaric-spin concept. If a plot is made of the known energy differences between the lowest-lying  $T=0$  state and the lowest  $T=1$  state *versus* mass number for the mass range 6 to 54, a consistent trend is seen. Interpolation on this plot suggests that in  $\text{Al}^{26}$  the lowest  $T=1$  state will be very near the lowest  $T=0$  state. In fact, it is possible that the ground state has  $T=1$ , as in the case<sup>2</sup> of  $\text{Cl}^{34}$ . Previous data on  $\text{Al}^{26}$  are inconsistent and leaves the energy and the isobaric spin of the ground state in doubt.<sup>1</sup>

The reaction  $\text{Si}^{28}(d,\alpha)\text{Al}^{26}$  is suitable for investigating the  $T=0$  levels of  $\text{Al}^{26}$  as it has an estimated  $Q$  value of 1 to 2 Mev. The deuteron, the alpha particle, and  $\text{Si}^{28}$  are all  $T=0$  nuclei; therefore, to the degree that isobaric spin-selection rules are valid, levels with  $T=1$  will not be observed.

The MIT-ONR electrostatic generator and associated high-resolution magnetic-analysis equipment have been used to study  $\text{Al}^{26}$  from its ground state to 2-Mev excitation. Fresh targets of natural  $\text{SiO}_2$  evaporated on thin Formvar backings were used. Because of low yield from this reaction, the targets used were of such thickness as to give an energy spread in the alpha groups several times the analyzer resolution. The alpha particles were observed at 90 degrees to the incident beam. Assignment of observed alpha groups to  $\text{Al}^{26}$  was based on observation of the change in alpha energy with a change in bombarding energy.

TABLE I. Reaction energies for the  $\text{Si}^{28}(d,\alpha)\text{Al}^{26}$  reaction.

$Q$ Value in Mev	Excitation of $\text{Al}^{26}$ in Mev
$1.416 \pm 0.008$	0
$0.998 \pm 0.008$	0.418
$0.364 \pm 0.008$	1.052
$-0.334 \pm 0.008$	1.750
$(-0.430) \pm 0.015$	(1.846)
$-0.648 \pm 0.008$	2.064

The results are given in Table I. Each  $Q$  value is the weighted average of at least three measurements made at bombarding energies ranging from 5 to 7 Mev. The excitation energy of  $\text{Al}^{26}$  given in the last column is based on the average ground-state  $Q$  value as shown. The 1.85-Mev level was completely resolved at only one bombarding energy. An accurate "energy shift" measurement was therefore not obtained. Thus, the assignment of this group to  $\text{Al}^{26}$  is not completely certain.

A region of about 3 Mev below the ground state has been covered with no indication of lower levels. An alpha of 10 percent of the intensity of the ground-state group would have been seen. No group of alphas from this reaction was seen between the listed ground state and the first excited state. At 6.5- and 7-Mev bombarding energy, the limit is about 3 percent of the intensity of the ground-state group.

Figure 1 shows the  $T=0$  energy levels of  $\text{Al}^{26}$  and their relation to reactions that have been studied elsewhere. Recent work of Haslam,<sup>3</sup> using the  $\text{Al}^{27}(\gamma,n)$  reaction and counting positrons from the  $\text{Al}^{26}$  decay as well as the neutrons, is in agreement with the presently

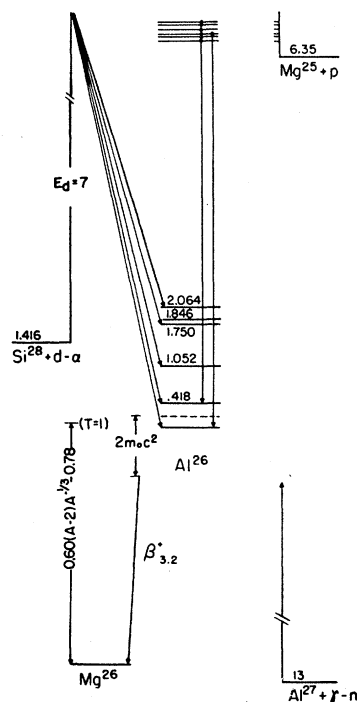


FIG. 1. Energy level scheme for  $\text{Al}^{26}$ . The levels up to 2 Mev are those observed in the present work. The calculated position of the lowest  $T=1$  level is shown. This is seen to coincide with the position given by the observed  $\beta^+$  decay end point. The  $\text{Al}^{27}(\gamma,n)$  threshold then agrees with the ground state. The high-lying levels are indicated by the resonances and gamma-ray energies observed by Kluver *et al.*